Gravity wave-driven flows in the solar tachocline

Kim, E. J. & MacGregor, K. B.

Original citation:
Kim, EJ & MacGregor, KB 2001, 'Gravity wave-driven flows in the solar tachocline' Astrophysical Journal, vol. 556, pp. L117–L120.
https://dx.doi.org/10.1086/322973

DOI 10.1086/322973
ISSN 0004-637X
ESSN 1538-4357

Publisher: American Astronomical Society

THE ASTROPHYSICAL JOURNAL, 556:L117–L120, 2001 August 1

GRAVITY WAVE–DRIVEN FLOWS IN THE SOLAR TACHOCLINE

EUN-JIN KIM[1] AND K. B. MACGREGOR
High Altitude Observatory, National Center for Atmospheric Research,[2] 3450 Mitchell Lane, Boulder, CO 80301
Received 2001 April 25; accepted 2001 June 22; published 2001 July 13

ABSTRACT

We present results from time-dependent hydrodynamic calculations of the interaction between internal gravity waves and the mean radial differential rotation in the solar tachocline. Such waves are thought to be generated by turbulent fluid motions at the base of the convection zone. Our simplified model treats the effects of wave forcing, produced by radiative damping of downward propagating disturbances, on the rotational shear flow in the region immediately below the convection zone. We have used the model to investigate the dependence of the computed flow properties on the values assumed for the wave frequency, the horizontal component of the wavevector, the initial wave velocity amplitude, and the viscosity of the background medium. Our results indicate that if the first three of these quantities are held fixed, stationary shear flow solutions are obtained for viscosities larger than a parameter-dependent critical value. If the viscosity is continuously decreased from this value, the flow undergoes a succession of dramatic transformations, first becoming periodic, then quasi-periodic, and ultimately chaotic when the viscosity is made sufficiently small. We discuss the implications of these results for the recently reported time variability of the angular velocity of rotation within the solar tachocline.

Subject headings: hydrodynamics — MHD — Sun: interior — Sun: magnetic fields — Sun: rotation — waves

1. INTRODUCTION

The apparent uniform rotation of the radiative core of the Sun, as revealed by recent analyses of measured *p*-mode frequency splittings (see, e.g., Charbonneau et al. 1998 and references therein), has renewed interest in the problem of angular momentum redistribution in the solar interior. One mechanism that has been proposed to explain the rotational state of the solar radiative interior is angular momentum transport and deposition by internal gravity waves (Kumar & Quataert 1997; Zahn, Talon, & Matias 1997). However, contrary to earlier expectations, recent work (Ringot 1998; Gough & McIntyre 1998; Kumar, Talon, & Zahn 1999; Kim & MacGregor 2001, hereafter KM) indicates that gravity waves cannot enforce uniform rotation within the solar interior, since they tend to accentuate shears rather than eliminate them. In particular, KM constructed stationary shear layer models in which such wave forcing was balanced by the force due to a prescribed viscosity. Depending on input parameter values, these models could exhibit complex vertical profiles in which the direction of the wave-driven horizontal flow alternated with increasing depth. This behavior was caused by the fact that the magnitude of the force produced by a prograde wave (i.e., one with horizontal propagation vector aligned along the direction of the ambient rotational shear flow) differs from that produced by an oppositely directed retrograde wave.

The purpose of this Letter is to extend the model developed in KM by incorporating a time-dependent description of the wave–mean flow interaction. Oscillatory shear flows driven by the interaction between gravity waves and a dissipative fluid have long been studied in the atmospheric sciences, in connection with the observed periodic reversal of the direction of the mean zonal winds in the equatorial stratosphere (i.e., the so-called quasi-biennial oscillation [QBO]; see, e.g., Plumb 1977 and references therein). In this Letter, we investigate whether the absorption of internal waves can similarly induce time variability of the radial differential rotation in the solar tachocline. To conduct this study, we utilize a conceptually simple hydrodynamic model in which the mean rotational flow is acted on by the force arising from the radiative damping of two gravity waves with opposite senses of horizontal propagation. Specifically, it is assumed that the waves are emitted from the bottom of the convection zone with identical frequencies and velocity amplitudes and with horizontal wavevector components that are equal in magnitude but oppositely signed; one wave is thus prograde, while the other is retrograde. We examine how the horizontal flow that is driven by these waves evolves in response to changes in the magnitude of the viscosity of the background fluid. We show that the time-dependent behavior of a flow that is produced in this way becomes increasing complex as the viscosity is decreased, evolving through stationary, periodic, and quasi-periodic states before eventually attaining a completely nonperiodic, chaotic state.

2. MODEL

We confine our attention to that portion of the radiative interior immediately below the convection zone. Within this region, the background distributions of density, pressure, temperature, and related quantities are represented using simple fits to the solar model of Bahcall & Pinsonneault (1995; see KM). Since the estimated width of the tachocline is $\ll R_\odot$, we adopt a Cartesian coordinate system in which the *x*- and *z*-axes are aligned along the azimuthal and (local) radial directions, respectively. We position the coordinate system such that the plane $z = 0$ coincides with the bottom of the convection zone and establish the layer $-H_0/2 \le z \le 0$ as our computational domain, where H_0 is the pressure scale height at the upper boundary. With $H_0 = 5.88 \times 10^9$ cm, the vertical extent of the domain is $\approx 0.04\ R_\odot$, comparable to the estimated radial thickness of the tachocline (e.g., Charbonneau et al. 1999).

Our model treats the interaction between the radial differential

[1] Current address: Department of Physics, University of California at San Diego, Urey Hall 7238, 9500 Gilman Drive, La Jolla, CA 92093-0319.

[2] The National Center for Atmospheric Research is sponsored by the National Science Foundation.

rotation in the tachocline, represented by a mean shear flow of the form $\boldsymbol{u} = u(z, t)\boldsymbol{e}_x$, and two hydrodynamic gravity waves, hereafter designated "+" and "−." These waves have frequencies $\omega_\pm = \omega$ and wavevectors $\boldsymbol{k}_\pm = \pm|l|\boldsymbol{e}_x + m_\pm \boldsymbol{e}_z$, so that the horizontal propagation of the $\pm$ wave is in the $\pm x$-direction. Under the Boussinesq and WKB approximations, ω and l are constants, and the wave dispersion relation yields $m_\pm = |l|[(N/\omega_\pm^*)^2 - 1]^{1/2}$, where $N(z)$ is the local Brunt-Väisälä frequency and $\omega_\pm^* = (\omega \mp |l|u)$. The vertical wavenumber $m_\pm$ thus varies with both depth and time through its dependences on N and u. We choose $m_\pm > 0$ to ensure that the vertical group velocity $v_{gz\pm} = -N|l|m_\pm/k_\pm^3$ is less than 0 and the waves travel downward from the convection zone base.

The coupled equations governing the time evolution of the wave-driven shear flow are

$$\rho \frac{\partial u}{\partial t} = \frac{|l|\mathcal{F}_+}{L_+} - \frac{|l|\mathcal{F}_-}{L_-} + \frac{\partial}{\partial z}\left(\rho\nu \frac{\partial u}{\partial z}\right), \tag{1}$$

$$\frac{\partial \mathcal{F}_\pm}{\partial z} = -\frac{\mathcal{F}_\pm}{L_\pm}, \tag{2}$$

where ρ and ν are background density and viscosity, $\mathcal{F}_\pm$ is the wave action density flux, and $L_\pm$ is the length scale for wave damping by the diffusion of radiation; in a medium with radiative diffusivity μ, $L_\pm = v_{gz\pm}/(\mu k_\pm^2)$. For waves with average total energy density $\langle E_\pm \rangle$, the action density and its flux are given by $\mathcal{S}_\pm = \langle E_\pm \rangle/\omega_\pm^*$ and $\mathcal{F}_\pm = v_{gz\pm}\mathcal{S}_\pm$, respectively. The first two terms on the right-hand side of equation (1) represent the force densities associated with the two waves. Note that because $v_{gz\pm} < 0$, both $\mathcal{F}_\pm$ and $L_\pm$ are less than 0, implying that the force produced by the $\pm|l|$ wave is in the $\pm x$-direction.

The viscosity ν appearing in the momentum equation (1) is a turbulent viscosity, attributed to the presence of weak, residual turbulence in the tachocline region that has a temporal and/or spatial scale that is larger than the scale of the gravity waves but smaller than the scale of the mean flow. Since the velocity amplitude of this turbulence is likely to be $\ll u$, we neglect its effect on the gravity waves. Note, moreover, that a term of the form $\partial S_\pm/\partial t$ has been omitted from the left-hand side of equation (2). By so doing, we assume that the wave propagation time through the domain is short in comparison to the timescale over which the flow evolves in response to the wave forcing (Plumb 1977). The inclusion of this term does not significantly alter the qualitative nature of the flow evolution derived from equation (2) (see § 4). Equations (1) and (2) together constitute a strongly nonlinear system since $L_\pm \propto (\omega_\pm^*)^4 = (\omega \mp |l|u)^4$; we therefore anticipate that $u(z, t)$ will exhibit complex time-dependent behavior.

The flow velocity $u(z, t)$ is obtained by numerical integration of equation (1) with the flux $\mathcal{F}_\pm(z, t)$ evaluated from equation (2) in the form

$$\mathcal{F}_\pm(z, t) = \mathcal{F}_{\pm 0} \exp\left[-\int_0^z dz'/L_\pm(z', t)\right], \tag{3}$$

where the subscript "0" indicates evaluation at the level $z = 0$. The flux at the upper boundary is given by $\mathcal{F}_{\pm 0} = \frac{1}{2}\rho_0 \delta v_{\pm 0}^2 m_{\pm 0}/l^2$, where $\delta v_{\pm 0}$ is the vertical (i.e., z-) component of the wave velocity. We assume that the specified quantity $\delta v_{\pm 0}$ has the same value of δv_0 for both waves and remains constant in time. Helioseismic inferences regarding the sense and magnitude of the change in angular velocity within the tachocline imply that the linear velocity difference across the shear layer at equatorial latitudes is $\sim 10^4$ cm s^{-1} with the bottom moving more slowly than the top. We therefore impose the boundary conditions $u(0, t) = 0$ and $u(-H_0/2, t) = -10^4$ cm s^{-1} on solutions of equation (1). This choice of upper boundary condition implies that $\omega_{\pm 0}^* = \omega$, $m_{\pm 0} = m_0$, and $\mathcal{F}_{\pm 0} = \mathcal{F}_0$.

3. FLOW EVOLUTION

We have used the computational model described in § 2 to derive solutions for gravity wave–driven shear flows corresponding to a wide range of values for the parameters ω, l, δv_0, and ν. In order to illustrate how flow properties evolve as the viscosity ν is varied, we consider a solution for which $\omega = 2 \times 10^{-3} N_0 = 5.02 \times 10^{-6}$ s^{-1}, $l = 1/H_0 = 1.70 \times 10^{-10}$ cm^{-1}, and $\delta v_0 = \omega/m_0 = 58.95$ cm s^{-1} (Press 1981). The adopted wave frequency corresponds to a period of about 2 weeks, comparable to the estimated timescales of fluid motions at the bottom of the convection zone. Because gravity waves of this frequency are strongly damped, they can affect the dynamics of the flow only to a depth $\sim 0.2H_0$. The different types of possible wave-driven flows are shown in Figure 1, wherein a synopsis of the behavior obtained for 10^8 cm^2 s^{-1} $\leq \nu \leq 3 \times 10^9$ cm^2 s^{-1} is presented.

The interplay between the wave and viscous forces is crucial to producing the time-dependent flow phenomena depicted in Figure 1. Near the upper boundary of the layer, the wave that propagates along the direction of the mean flow damps more rapidly, a consequence of the velocity dependence of the radiative damping length (see § 2). The force arising from the dissipation of this wave is therefore larger than that contributed by its oppositely traveling counterpart, leading to a net wave force that acts to enhance the shear present in the mean flow. At somewhat greater depths, this preferential damping process reduces the flux of the principal force-producing wave to the point that the other wave becomes dominant, causing both the net wave force and the mean flow to reverse direction. Note, however, that this tendency for gravity wave interactions to create and accentuate regions of strong shear is mitigated by the ability of viscous diffusion to smooth and dissipate these flow structures. In view of the competing dynamical roles played by viscous and wave forces, we expect that the nature of solutions to the strongly nonlinear system consisting of equations (1) and (2) should depend on the ratio $\nu/\mathcal{F}_0$ and that the progression through a sequence of instabilities toward possible chaotic behavior should occur as the value of this ratio is decreased. This expectation is confirmed by the results presented in Figure 1.

For values of the viscosity larger than 3×10^9 cm^2 s^{-1}, gravity wave forcing of the background fluid drives a stationary shear flow, analogous to the time-independent solutions found by KM. In these cases, after an initial phase of transient relaxation, the velocity u assumes an equilibrium profile throughout the domain, with the horizontal force arising from the wave–mean flow interaction balanced by the viscous force at each depth. For $\nu = 3 \times 10^9$ cm^2 s^{-1}, the flow begins to manifest time-dependent behavior, the wave-induced horizontal motion of the fluid becoming oscillatory with a single, well-defined period. As in the QBO, the periodic character of the motion near the bottom of the convection zone results from the upward propagation of the two oppositely directed shear

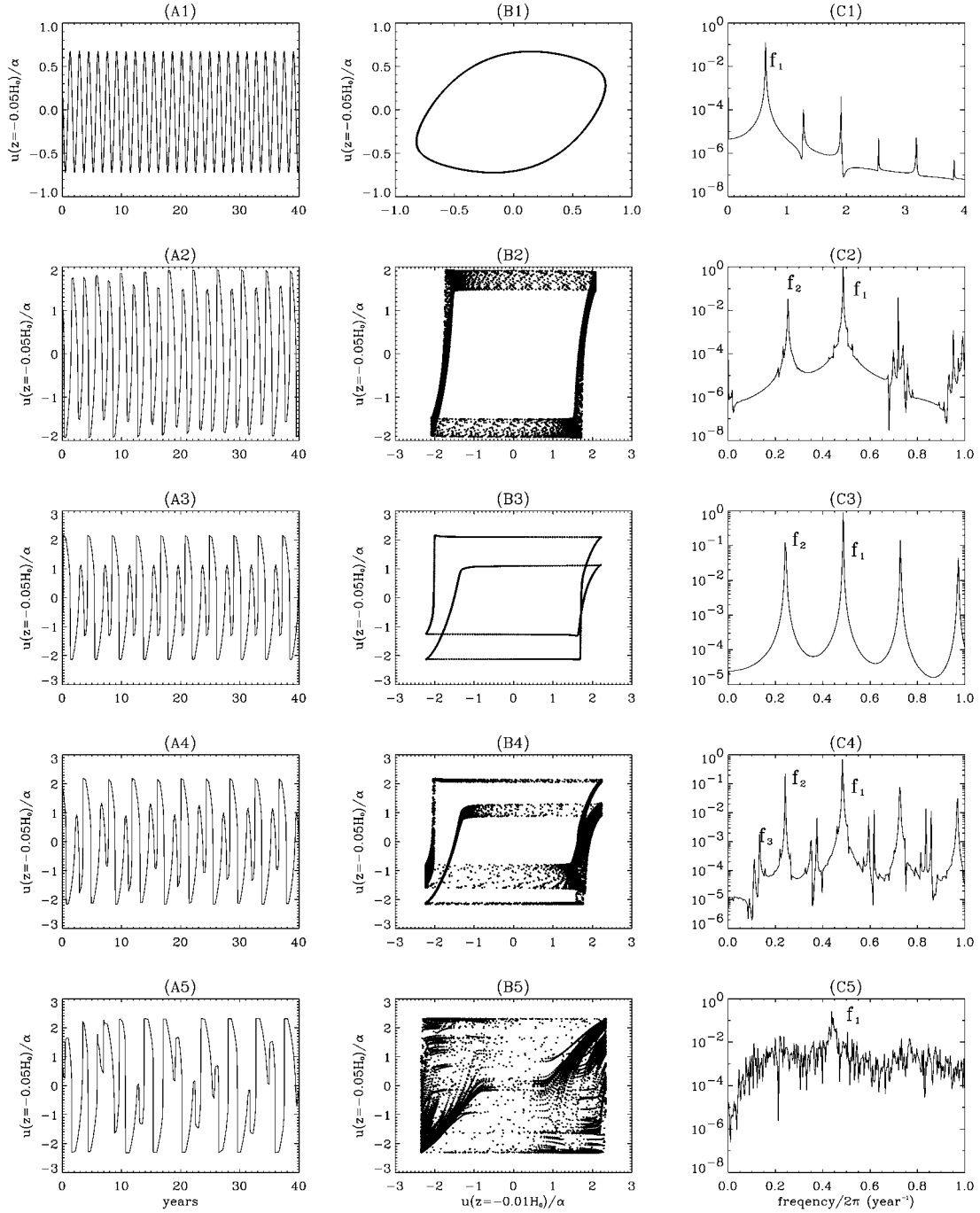

FIG. 1.—(A1–A5) Time evolution of the mean flow velocity u at $z = -0.05H_0$, (B1–B5) the phase space constructed by time history of u at two distinct spatial points, $z = -0.01H_0$ and $-0.05H_0$, and (C1–C5) frequency power spectrum of u at $z = -0.01H_0$; u is normalized by the amplitude of the velocity at the lower boundary $\alpha \equiv 10^4$ cm s^{-1}. For each of the rows in the figure, the corresponding values of the viscosity are 3×10^9 cm^2 s^{-1} (A1–C1), 5×10^8 cm^2 s^{-1} (A2–C2), 3×10^8 cm^2 s^{-1} (A3–C3), 2.8×10^8 cm^2 s^{-1} (A4–C4), and 10^8 cm^2 s^{-1} (A5–C5).

zones located just below $z = 0$ (e.g., Plumb 1977). This apparent phase propagation is produced by viscous diffusion across the internal shear layer between these two counterflowing regions. The oscillatory nature of this shear flow can be seen in Figure 1, where the time evolution of u at the fixed position $z = -0.05H_0$ is plotted in panel A1. The periodic behavior of u can also be seen in a phase-space diagram constructed from the time history of u at two different spatial points, $z = -0.01H_0$ and $-0.05H_0$ (panel B1). The period of the oscillation can be determined accurately from the frequency power spectrum shown in panel C1, which is obtained by taking the Fourier transform of a long time series of $u(-0.01H_0, t)$. It is clearly seen there that the power spectrum contains peaks at frequencies that are integer multiples of the basic frequency $f_1 = 2\pi/1.580$ yr^{-1}. An investigation of the first (Hopf) bifurcation marking the transition from a stationary to periodic gravity wave–driven flow was first conducted by Yoden & Holton (1988), within the context of models for the QBO in the terrestrial atmosphere.

As the viscosity is further decreased, the original frequency

f_1 gradually decreases. When $\nu = 5 \times 10^8$ cm^2 s^{-1}, a second frequency, $f_2 = 2\pi/3.952$ yr^{-1}, appears in the power spectrum, having a value that is incommensurate with the first (now $f_1 = 2\pi/2.058$ yr^{-1}); the appearance of this second frequency indicates the onset of quasi-periodic fluid motions. The quasi periodicity is evident in panel B2, where the projection of a two-dimensional torus can be seen. The frequencies of all of the peaks present in the power spectrum of panel C2 can be expressed as linear combinations of f_1 and f_2. Continued reduction of the value of ν causes f_1 to increase but f_2 and the ratio f_2/f_1 to decrease; the next significant transition occurs when $\nu = 3 \times 10^8$ cm^2 s^{-1}, for which $f_1 = 2\pi/2.057$ yr^{-1} and $f_2/f_1 = \frac{1}{2}$. The commensurability of f_1 and f_2 for this value of the viscosity marks the evolution of the flow into a state of phase locking and the return of periodic motion at a frequency $f_2 = f_1/2$, as seen in panels A3 and B3. Strong peaks at multiples of this frequency are prominent in the power spectrum shown in panel C3.

For decreasing ν in the range 2.8×10^8 cm^2 s$^{-1} < \nu \leq 3 \times 10^8$ cm^2 s^{-1}, both the frequencies f_1 and f_2 steadily decrease but remained phase-locked with $f_2 = f_1/2$. When $\nu = 2.8 \times 10^8$ cm^2 s^{-1}, a third frequency, f_3, appears in the power spectrum (panel C4), having a value $f_3 = 2\pi/7.482$ yr^{-1} that is incommensurate with the preexisting frequencies $f_1 = 2f_2 = 2\pi/2.070$ yr^{-1}. At this point, the wave-driven fluid motions revert to quasi-periodic behavior, as is apparent from inspection of panels A4–C4. The final transition in the sequence of instabilities that characterizes the flow evolution occurs when the viscosity attains the value $\nu = 10^8$ cm^2 s^{-1} and u becomes chaotic. The onset of nonperiodic fluid motion is indicated by the disappearance of the two-dimensional torus in going from the phase-space diagram of panel B4 to that of panel B5, as well as from the broad, continuous spectrum containing no sharp peaks that is displayed in panel C5. Note that despite the flow having undergone a transition to chaos, the frequency f_1 can still be recognized in the power spectrum of panel C5.

4. SUMMARY AND DISCUSSION

We have conducted a systematic investigation of the time-dependent behavior of shear flows driven by low-frequency internal waves in the stably stratified layers just beneath the solar convection zone. Such waves are subject to vigorous radiative damping and are thereby capable of interacting with the mean shear flow arising from the radial differential rotation that is known to exist within the tachocline region. Depending on the magnitude of the turbulent viscosity appropriate to the outer layers of the Sun's radiative interior, wave–mean flow interactions of this kind can have a variety of different consequences for the dynamical state of the shear layer. For a particular set of wave and fluid parameter values, we have shown that for decreasing ν in the range 10^8 cm^2 s$^{-1} \leq \nu \leq 3 \times 10^9$ cm^2 s^{-1}, computed flow solutions evolve through a sequence of instabilities (i.e., bifurcations) marking successive transitions between stationary, periodic, quasi-periodic (two frequencies), periodic (phase-locked), quasi-periodic (three frequencies), and chaotic states. This type of evolution is characteristic of strongly nonlinear dynamical systems, bearing a close resemblance, for example, to the progression of behaviors leading to turbulence in laboratory experiments on convection in fluids (e.g., Gollub & Benson 1980).

Results obtained for values of ω, l, and δv_0 other than the ones considered here indicate that the flow evolution in response to changing ν follows the same qualitative pattern as outlined above, albeit within different ranges of ν-values. Additional information concerning the detailed parameter dependences of gravity wave–driven flow properties will be provided in a subsequent paper, including the effects of a uniform horizontal magnetic field in the tachocline. Likewise, preliminary results derived using a model in which the explicit time dependence of the wave action density is retained suggest that the system follows a path to chaotic behavior that is generally similar, except that the transitions described previously occur for somewhat larger values of ν.

The results presented in § 2 are especially interesting in the light of recent efforts to observe time variations in the angular velocity of rotation of a portion of the solar interior in the vicinity of the tachocline. In particular, based on their analysis of 4 years worth of helioseismic observations from the Global Oscillation Network Group and the Michelson Doppler Imager, Howe et al. (2000) have reported detecting small-amplitude, periodic changes in the equatorial rotation rate of a layer located near the base of the convection zone ($r = 0.72\ R_\odot$). Although these measurements and the 1.3 yr period inferred from them have yet to be validated (see Antia & Basu 2000), given the range of complex, time-variable flows that can be produced by gravity wave interactions, additional investigations utilizing longer duration helioseismic data sets seem warranted.

We thank G. Barnes and P. H. Diamond for helpful discussions and H. Liu for a careful reading of and useful comments on the manuscript. E.-J. K. was supported in part by the US Department of Energy under grant FG03-88ER 53275.

REFERENCES

Antia, H. M., & Basu, S. 2000, ApJ, 541, 442
Bahcall, J. N., & Pinsonneault, M. H. 1995, Rev. Mod. Phys., 67, 781
Charbonneau, P., Christensen-Dalsgaard, J., Henning, R., Larsen, R. M., Schou, J., Thompson, M. J., & Tomczyk, J. 1999, ApJ, 527, 445
Charbonneau, P., Tomczyk, S., Schou, J., & Thompson, M. J. 1998, ApJ, 496, 1015
Gollub, J. P., & Benson, S. V. 1980, J. Fluid Mech., 100, 449
Gough, D. O., & McIntyre, M. E. 1998, Nature, 394, 755
Howe, R., Christensen-Dalsgaard, J., Hill, F., Komm, R. W., Larsen, R. M., Schou, J., Thompson, M. J., & Toomre, J. 2000, Science, 287, 2434
Kim, E., & MacGregor, K. B. 2001, ApJ, submitted (KM)
Kumar, P., & Quataert, E. J. 1997, ApJ, 475, L143
Kumar, P., Talon, S., & Zahn, J.-P. 1999, ApJ, 520, 859
Plumb, R. A. 1977, J. Atmos. Sci., 34, 1847
Press, W. H. 1981, ApJ, 245, 286
Ringot, O. 1998, A&A, 335, L89
Yoden, S., & Holton, J. R. 1988, J. Atmos. Sci., 45, 2703
Zahn, J.-P., Talon, S., & Matias, J. 1997, A&A, 322, 320